HIGH-SENSITIVITY INTRACAVITY LASER SPECTRUM ANALYZER OPERATING IN THE WAVELENGTH REGION 770–820 nm

A.N. Kolerov

All-Union Scientific-Research Institute of Physico-Technical and Radio-Technical Measurements, Moscow
Received December 25, 1989

The sensitivity of an intracavity laser spectrometer was increased by two orders of magnitude in the near-IR ($\Delta\lambda \sim 770$–820 nm). *Using this spectrometer, 132 new absorption lines were recorded in this spectral interval, which is normally considered to be an atmospheric transmission window.*

An intracavity laser (ICL) spectrum analyzer, based on a Cr^{3+}: GSGG laser,[1] sensitive to absorption coefficients κ as low as $\sim 10^{-6}$ cm^{-1}, has made it possible to record absorption lines in the range of $\Delta\lambda \sim 770$–820 nm. This spectral range is one of the "transmission windows" of the atmosphere, and instrumentation with high sensitivity is needed for a detailed analysis of the fine structure of these lines. Earlier,[2] using a spectrum analyzer based on a Ti^{3+}: Al_2O_3 laser, it became possible to increase the sensitivity of ICL spectroscopy in this range down to $\kappa \sim 10^{-8}$ cm^{-1}. However, this laser has a number of special features which complicate its use in these measurements (a short lifetime of excitation $\tau \sim 4$ μs, the necessity of using a "spectral transformer"[2] with flashlamp pumping, etc.). In this paper, therefore, the possibility is considered of achieving a higher sensitivity of the ICL spectrum analyzer based on a quasicontinuous Cr^{3+}: GSGG laser.

The optical block diagram of the experimental setup is shown in Fig. 1. The basis of the laser crystal was GSGG: Cr^{3+} 6 mm in diameter and 65 mm in length, placed in a quartz silvered reflector cooled liquid refrigerant with the additives R6G and OX-17 organic dyes. The crystal was excited one or two xenon lamps with maximum energy of electrical pumping $W \le 2$ kJ. To obtain a resonator configuration close to confocal, spherical mirrors were used (or flat in combination with ordinary ones, and also weakly absorbing lenses). The spectral reflection coefficients of the mirrors were 100% in the range $\Delta\lambda \sim 700$–900 nm.

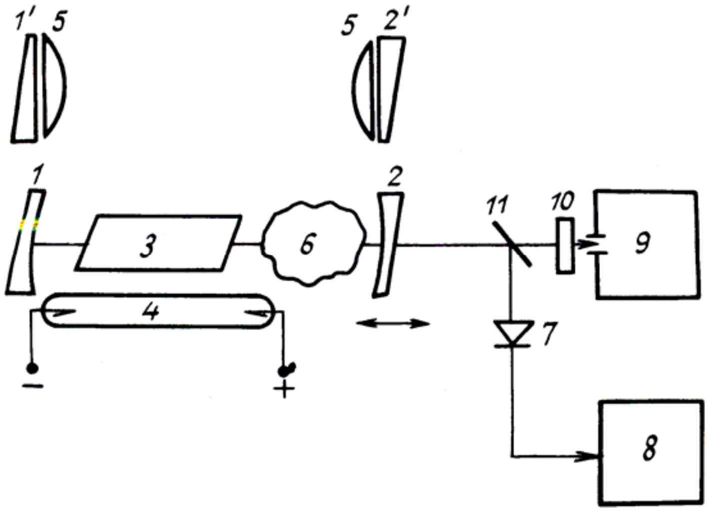

FIG. 1. Optical block diagram of the setup: 1, 2 – resonator mirrors; 3 – active medium; 4 – xenon lamp; 5 – lenses; 6 – investigated object; 7 – photodetector; 8 – recording oscilloscope; 9 – spectrograph; 10 – light filters; 11 – lightsplitter.

The selection of the wavelength interval of operation of the spectrum analyzer was accomplished by substituting mirrors with the corresponding spectral reflection coefficients. The kinetics of pulse generation was recorded by a photodetector connected to a recording oscilloscope. This made it possible to experimentally record the value of the duration of quasicontinuous generation, which finally determines the sensitivity of the ICL spectrum analyzer. The laser emission spectrum was recorded on I-810 film behind the spectrograph ($R \sim 6 \cdot 10^5$, $D \sim 1$ nm/cm). To eliminate possible parasitic flare spots, S3S-20 and KS-19 filters, which cut off radiation below 720 nm, were mounted at the input of the spectrograph.

The main results obtained in there experiments were the following. In the free generation mode of the laser, the duration of an individual spike did not exceed 1–3 μs with the total pulse duration on the order of 150–200 μs. The maximum possible sensitivity of the spectrum analyzer in this case, allowing for 20% resolution of the absorption line, did not exceed $\sim 3 \cdot 10^{-6}$ cm^{-1} (Ref. 1). Change of the base length ($L \sim 0.5$–1 m) of the cavity and the pumping rate, as in Refs. 2 and 3, led to a transformation from the free generation mode to quasicontinuous generation. This, in its turn, caused an increase in the pulse duration of quasicontinuous generation and an increase in the sensitivity of the ICL spectrum analyzer.

As the cavity configuration was changed bringing it closer to a confocal one, the depth of the amplitude pulsations of the generation pulse changed and it became possible to record weaker and weaker atmospheric absorption lines in the emission spectrum (see Fig. 2). For an amplitude pulsation depth (Δ) of $\sim$ 30–40%, it was possible to record absorption lines whose sensitivity of detection was lower than the values $\kappa \sim 5 \cdot 10^{-8}$ cm^{-1} listed in the atlases.[4,5] For $\Delta \sim$ 15–20%, a number of absorption lines, lacking in the atlases,[4,5] were recorded, which testifies that the ICL spectrum analyzer is capable of a sensitivity of $\kappa \sim 10^{-8}$ cm^{-1}. The absorption lines corresponding to the spectra in Fig. 2 are listed below (identification of known lines is given in Refs. 4 and 5). 132 new absorption lines were recorded within a rather small range ($\Delta\lambda \sim 8$ nm). Thus, this spectrum analyzer may find application in analytical spectroscopy.

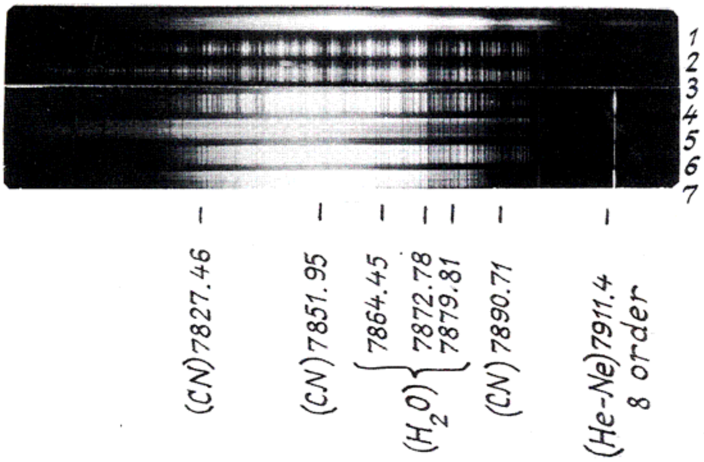

FIG. 2. Fragments of absorption spectra with 1) $\Delta \sim 100\%$ ($\kappa \sim 10^{-6}$ cm^{-1}), *2)* $\Delta \sim 10\%$ ($\kappa \sim 10^{-8}$ cm^{-1}), *3)* $\Delta \sim 20\%$ ($\kappa \sim 3 \cdot 10^{-8}$ cm^{-1}), *4)* $\Delta \sim 40\%$ ($\kappa \sim 8 \cdot 10^{-8}$ cm^{-1}), *5)* $\Delta \sim 60\%$ ($\kappa \sim 10^{-7}$ cm^{-1}), *6)* $\Delta \sim 80\%$ ($\kappa \sim 5 \cdot 10^{-7}$ cm^{-1}), 7) $\Delta \sim 90\%$ ($\kappa \sim 8 \cdot 10^{-7}$ cm^{-1}).

789.637		789.369	CN	789.101	H_2O	788.712	H_2O	788.346	
789.602	H_2O	789.348	H_2O	789.071	CN	788.682	H_2O	788.309	CN
789.581		789.311		788.997		788.623	H_2O	788.290	CN
789.555	H_2O	789.284	CN	788.941	H_2O	788.574		788.233	CN
789.513	CN	789.249		788.907		788.528	CN	788.210	CN
789.486	H_2O	789.212	CN	788.882	H_2O	788.505	H_2O	788.930	H_2O
789.451		789.187	H_2O	788.847		788.446	CN	788.163	
789.412	CN	789.161		788.815		788.422		788.089	
789.407	CN	789.111	H_2O	788.779	CN	788.361	CN	788.073	H_2O
788.040	CN	786.908		785.807		784.661		783.178	
787.987	H_2O	786.861	CN	785.750		784.627	H_2O	783.150	
787.935		786.818		785.703		784.591		783.098	
787.895	CN	786.803		785.663		784.551		783.077	CN
787.871		786.759	CN	785.647		784.514		783.046	
787.829		786.733	CN	785.596		784.484		783.009	

787.811		786.702		785.559		784.444		782.971	
787.780		786.667	H_2O	785.506		784.357		782.925	
787.734		786.608	H_2O	785.467		784.260		782.893	
787.709	CN	786.567		785.437	CN?	784.209		782.847	
787.671	H_2O	786.515		785.401	H_2O	784.174		782.746	CN
787.653	H_2O	786.494		785.379		784.152		782.702	
787.608	H_2O	786.469		785.346		784.113		782.635	CN
787.589	CN	786.445	H_2O	785.313		784.053		782.606	
787.531	H_2O	786.428		785.255		784.015		782.583	
787.990	CN	786.375		785.229		783.962	H_2O	782.561	
787.450		786.375		785.195	CN	783.895		782.521	
787.433		786.321	H_2O	785.171		783.880		782.453	
787.405		786.309		785.145		783.837		782.418	CN
787.395	CN	786.270		785.129		783.811		782.387	
787.337	CN	786.236		785.087		783.777		782.321	
787.301		786.206		785.049	CN	783.740		782.298	
787.278	H_2O	786.188	CN?	785.029	CN	783.709		782.177	CN
787.265	CN	786.127		785.995	CN	783.670	CN	782.125	
787.201		786.104		785.938		783.643		782.074	
787.168		786.076	H_2O	785.903	CN	783.578	CN?	782.041	
787.141		786.015		784.875	H_2O	783.562	CN	781.965	
787.114		785.983		784.847		783.460	CN	781.950	
787.056	H_2O	785.947	CN	784.838		783.414		781.923	
787.009		785.915		784.797		783.374		781.902	
786.991	H_2O	785.882	CN	784.764	CN?	783.351		781.857	
786.962		785.849		784.735		783.314		781.817	
786.950		785.826		784.691		783.251		781.724	CN

Note: wavelength in nm.

REFERENCES

1. E.V. Zharikov, A.N. Kolerov, V.V. Laptev, et al., Dokl. Akad. Nauk SSSR **285**, No. 1, 92 (1985).
2. A.N. Kolerov, Zh. Prikl. Spectrosk. **44**, No. 3, 363 (1986).
3. A.N. Kolerov, Zh. Prikl. Spectrosk. **45**, No. 1,135 (1986).
4. J.W. Swenson, W.S. Benedict, J. Delboulle, et al., *The Solar Spectrum from λ7498 to λ2016*, Liege (1970).
5. C.E. Moore, M.G.J. Minneart, and J. Hautgast, *The Solar Spectrum from λ2935 to λ8770*, NBS Monograph 61, Washington (1966).